ChemComm

COMMUNICATION

View Article Online
View Journal | View Issue

Cite this: *Chem. Commun.*, 2025, 61, 4824

Received 25th January 2025,
Accepted 21st February 2025

DOI: 10.1039/d5cc00466g

rsc.li/chemcomm

Hybrid films of novel fluorinated polyimides and hyperbranched cyclotriphosphazene polymer for enhanced flame retardancy, thermomechanical properties, and reduced dielectric constant†

Sivagangi Reddy Nagella and Chang-Sik Ha *

This study synthesizes novel polyimide (B2FO PI) films using 4,4′-(1,4-phenyleneisopropylidene)diphenoxy bis(2-(trifluoromethyl)-4-aminobenzene) (B2FDA) and 4,4′-oxydiphthalic anhydride (ODPA), as well as polyimide (PI) hybrid films incorporating a hyperbranched fluorinated cyclotriphosphazene polymer. The findings indicate that incorporating the hyperbranched cyclotriphosphazene significantly enhances the hybrid films' performance by increasing the cross-linking density of the polyimide chains. Moreover, the hybrid PI films demonstrate excellent water resistance, superior thermomechanical properties, enhanced flame-retardant characteristics, and a low dielectric constant.

Organic/inorganic polyimide (PI) hybrids have gained increasing significance due to their exceptional performance characteristics. These hybrids combine the processability and flexibility of the thermally stable organic PI matrix with the enhanced mechanical properties of inorganic fillers. By incorporating rigid, high-surface-area materials such as silica, metal oxides, and phosphazene nanoparticles through surface functionalization, these hybrids enhance the mechanical and thermal properties of the PI matrix.[1–4]

Phosphazene-polyimide hybrids represent an advanced class of organic–inorganic materials, garnering significant attention for their seamless integration of the strengths inherent in both components.[5–8] These hybrids are based on hexachloro cyclotriphosphazene (HCP), a cyclic molecule composed of alternating phosphorus and nitrogen atoms, each phosphorus atom bearing two chlorine substituents. HCP is renowned for its exceptional thermal properties, including flame retardancy and self-extinguishing behavior in its polymeric form. Additionally, HCP offers remarkable versatility in synthesis, facilitating the preparation of copolymers with diverse substituents and excelling across a broad range of molecular weights. This unique combination of properties positions phosphazene-PI hybrids as a versatile and innovative platform, enabling the development of high-performance materials tailored to the stringent requirements of advanced applications.[9]

Polydichlorophosphazene, first synthesized by Stokes in the 19th century *via* $[PNCl_2]_3$ ring-opening polymerization, was initially overlooked due to instability. However, In the mid-1960s, Allcock and Kugel significantly advanced its potential by precisely controlling the ring-opening polymerization of $[PNCl_2]_3$, yielding a soluble, uncrosslinked linear polymer with enhanced thermal stability, flame retardancy, and customizable functionalities, enabling a broader range of applications.[10] For instance, HCP based PI-epoxy resin 3D interpenetrating polymer network (IPN) improved flame retardancy, mechanical properties, while reducing the dielectric constant (ε) of PI hybrids.[11] In another study, bismaleimide composites based on linear polyphosphazene (LPZ) demonstrated that when the LPZ content increased from 0–4%, the limiting oxygen index (LOI) increased from 31% to 34.5%, while the ε lowered from 3.19 to 2.67 at 1 MHz.[12] Beyond flame-retardant uses, polyphosphazenes are increasingly applied in biomedical fields, energy storage systems, environmental applications, and high-performance coatings for industries such as aerospace and electronics.[3,4] Their versatility and capacity for customization make them ideal for a wide range of advanced applications.

This communication reports the synthesis of novel hyperbranched polyphosphazenes and their hybrids with B2FO PIs. Additionally, the thermal, mechanical, optical, water resistance, dielectric properties, and flame retardancy of the hybrid films were investigated. The synthetic route and chemical structure of the soluble hyperbranched poly[cyclotriphosphazene-*co*-(4,4′-(perfluoropropane-2,2-diyl)diphenol)] (CPAF) are described, with proton nuclear magnetic resonance (^{1}H NMR) spectroscopic analysis provided in Fig. S1b (ESI†). The reaction was performed in acetonitrile at room

Department of Polymer Science and Engineering, School of Chemical Engineering, Pusan National University, Busan 46241, Korea. E-mail: csha@pnu.edu

† Electronic supplementary information (ESI) available: Details of experimental details, syntheses, ^{1}H NMR spectra, UV-visible spectra, WAXD diffraction patterns, WCA and PWA, and surface SEM images with EDS patterns, and digital images of key materials. Representative DMA thermograms of B2FO PI and B2FO-CPAF PI hybrid films before and after flame exposure. See DOI: https://doi.org/10.1039/d5cc00466g

temperature in an ultrasonic bath, using triethylamine (TEA) as an acid acceptor. TEA accelerated the nucleophilic replacement between the terminal hydroxy group and P–Cl bonds, resulting in the formation of hyperbranched polymers with an excess of bisphenol-AF (BPAF). The diamine monomer B2FDA was synthesized following previously reported methods, with ^{1}H NMR Spectroscopy shown in Fig. S2 (ESI†).[13] B2FO PI was synthesized using a conventional two-step process, beginning with the ring-opening polyaddition of B2FDA and 4,4′-oxydiphthalic anhydride (ODPA) in *N*-methyl pyrrolidone (NMP) at room temperature to form poly(amic acid) (PAA). The PAA was then subjected to chemical imidization using Ac_2O/Py as the dehydrating agent at 60 °C, resulting in the final polyimide structure, as confirmed by the ^{1}H NMR spectroscopy presented in Fig. S3 (ESI†). For the synthesis of B_2FO-CPAF hybrids, B2FDA was dissolved in anhydrous NMP, followed by the addition of a slight excess of ODPA, and the mixture was stirred under nitrogen for 6 h. The resulting PAA underwent chemical imidization with Ac_2O/Py at 60 °C to form the polyimide. Subsequently, CPAF was introduced into the resulting PI solution and stirred for an additional 2 h. The resin solution was cast onto glass plates and thermally cured to produce B_2FO-CPAF hybrid PI films. The synthetic route and chemical structure of fluorinated PI and its hybrids are depicted in Scheme 1.

Fig. S4 (ESI†) illustrates the Fourier transform infrared (FTIR) spectra. The HCP structure is evident from the broad peak at 1180 cm^{-1}, attributed to the asymmetric P–N–P stretching, and the peak at 873 cm^{-1}, corresponding to symmetric P–N–P stretching. The P–Cl bond, observed with peaks at 594 cm^{-1} and 505 cm^{-1}, diminished after reacting with BPAF.[14] For BPAF, absorption peaks at 1616 cm^{-1} and 1515 cm^{-1} are assigned to the phenyl groups of the BPAF units, while the characteristic peaks of the –CF_3 group are observed at 1209 cm^{-1} and 1174 cm^{-1}.[15] Similarly, the FTIR spectrum of CPAF confirms the presence of phenyl groups in the hexafluoroisopropylidene diphenol units (absorption bands at 1616 cm^{-1} and 1515 cm^{-1}), and the –CF_3 group (1209 cm^{-1} and 1174 cm^{-1}), along with the characteristic P–N stretching band at 876 cm^{-1}. Additionally, the broad absorption peak for the phenolic hydroxyl group of BPAF, initially observed between 3290–3470 cm^{-1}, shifts to longer wavelengths after polycondensation. This shift indicates that the phenolic hydroxyl groups are free from hydrogen bonding and are dispersed within the hyperbranched CPAF polymer. Based on this analysis, it can be concluded that the product incorporates structural units of both HCP and BPAF. Furthermore, a comparison of CPAF and pure PI with the B2FO-CPAF hybrid reveals an enhancement in the intensity of the 1616 cm^{-1} peak, attributed to the incorporation of CPAF.

The structural properties of the films were successfully investigated using FTIR spectroscopy. To further examine the miscibility of the PI matrix with hyperbranched CPAF, optical transparency and wide-angle X-ray diffraction (WAXD) analyses were conducted. Similar to previously reported PI films of 4,4′-(1,4-phenyleneisopropylidene)diphenoxy bis(2-(trifluoromethyl)-4-aminobenzene) with 4,4′-(hexafluoroisopropylidene)diphthalic anhydride (FDA) or 1,2,3,4-cyclobutanetetracarboxylic dianhydride (CBDA),[13] the novel B2FO films exhibit high transparency in the visible region (Fig. S5 and Table S1, ESI†). However, the incorporation of CPAF results in reduced transparency, attributed to the microphase separation in the PI hybrids, despite the effective molecular-level distribution of CPAF within the PI matrix through covalent bonding. To ensure uniform dispersion and understand the observed microphase separation, WAXD analysis was performed (Fig. S6, ESI†). The WAXD patterns confirm the amorphous nature of hybrid films. Notably, the amorphous maxima ($2\theta \approx 18^\circ$) shifts to lower angles with increasing CPAF content, indicating an increase in *d*-spacing. This shift suggests the intercalation of hyperbranched CPAF, leading to the separation of PI chain segments, which contributes to the reduced transparency and increased opacity of the hybrid films.

Thermogravimetric analysis (TGA) curves of the PI hybrids revealed that their thermal behavior was closely linked to the CPAF loading, with a notable change occurring at 1 wt% and 4 wt% (Fig. 1a). This variation is attributed to the lower thermal stability of CPAF, which, despite degradation at 380 °C, contributes to an increased char yield or residual weight ratio at

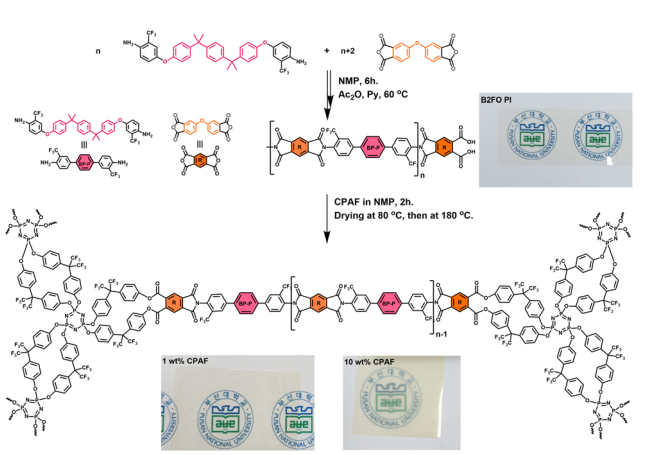

Scheme 1 Synthesis and structures of the B2FO PI and B2FO-CPAF hybrids.

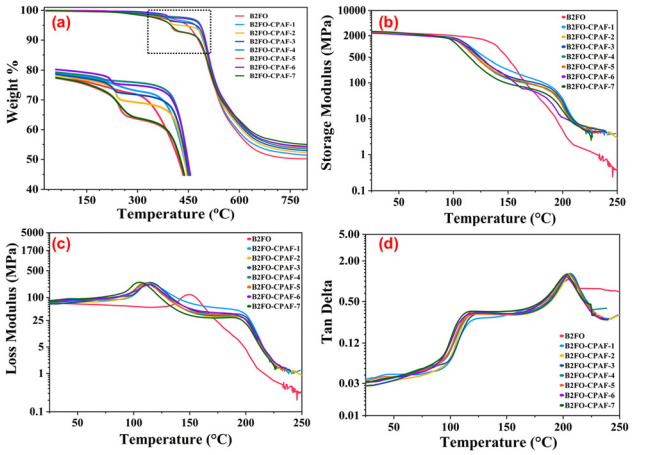

Fig. 1 TGA curves (a) DMA thermograms (b)–(d) of B2FO PI and B2FO-CPAF PI hybrid films.

700 °C (R_w^{700}), as shown in Table S1 (ESI†). This improvement results from the formation of thermally stable, flame-retardant P–O–P polymer chains derived from the P–N–P chains.[9] Additionally, the exothermic glass transition temperature (T_g) values (Table S1, ESI†) of the PI hybrids increased slightly, from 208 °C for pure PI to 217 °C for CPAF-7. This increase is likely due to the crosslinking of the flexible PI chains with the free hydroxyl groups of the CPAF hyperbranched polymer, leading to a stronger PI network. The enhanced network structure is further supported by the observed increase in tensile strength and modulus in the hybrids compared to the pure PI films.

Water resistance is crucial for achieving low dielectric properties in PI films. To evaluate these properties, static water contact angle (WCA) measurements and percentage water absorption (PWA) studies were performed for both PI and hybrid films, with results presented in Table S2 (ESI†) (Fig. 2). The data show a consistent increase in WCA with the addition of CPAF, attributed to its intrinsic hydrophobicity. This hydrophobic nature reduces the surface tension of the hybrid films, improving their water resistance. The PWA results, shown in Fig. 2, indicate that incorporating CPAF effectively reduces water absorption, directly resulting from the increased hydrophobicity. The enhanced hydrophobic properties and improved compatibility between PI and CPAF suggest that the resulting hybrids are well-suited for low dielectric applications.

The incorporation of CPAF into the PI matrix enhances the flame retardancy of the hybrid films, as demonstrated by increased LOI values. In the case of B2FO, the flame continued to burn even after the external flame source was removed.[16] However, this tendency decreased with increasing CPAF content. Fig. S8 (ESI†) shows the films before and after flame exposure. After combustion tests, the samples (B2FO: 0% CPAF, B2FO-CPAF-3: 2% CPAF, and B2FO-CPAF-7: 10% CPAF) exhibited black, tough char layers, with higher CPAF content resulting in greater char formation. This increased char serves as a combustion barrier. Additionally, a thick, compact char layer is known for its ability to protect the internal structure from flame exposure and reduce the release of flammable gases. To better understand the role of residual char layers in influencing the combustion behavior of the films, the micro-morphology and elemental composition of the char layers were analysed post-combustion (Fig. S7b–g, ESI†). The results confirm that adding CPAF significantly improves flame retardancy, as indicated by the higher LOI values.

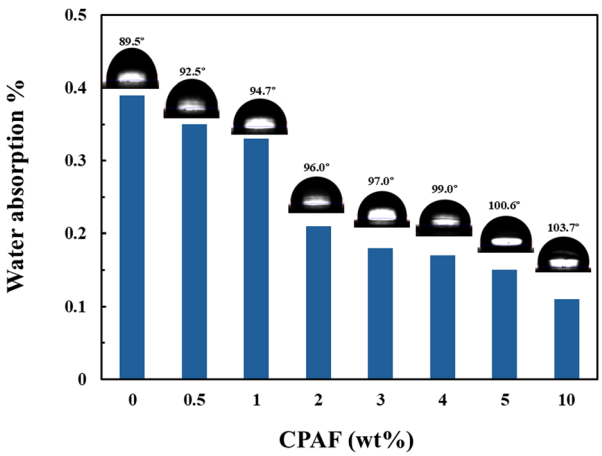

Fig. 2 WCA and PWA of B2FO PI and B2FO-CPAF PI hybrid films.

Tensile strength is a key indicator of the mechanical properties of PI and hybrid films. The influence of CPAF content on tensile strength is shown in Fig. S9 (ESI†) and summarized in Table S2 (ESI†), based on tensile tests conducted at room temperature. The results demonstrate that tensile strength increases with CPAF content, reaching a peak of 71.9 MPa at 10 wt% CPAF, representing a 38% improvement over the neat PI tensile strength of 52.1 MPa. The tensile modulus also increased from 2.4 to 3.3 GPa. This enhancement is attributed to the uniform dispersion of CPAF and its strong covalent bonding with the PI matrix, which effectively strengthens the hybrid structure. However, while the incorporation of CPAF improves certain properties, it also leads to the formation of a network structure that negatively impacts elongation at break. The elongation at break of the PI-hybrid films decreases progressively with increasing CPAF content. This reduction is likely due to higher cross-linking density and stronger intermolecular interactions within the hybrid films, limiting their ability to deform under stress. As a result, the toughness of the composites decreases with higher CPAF content, leading to earlier fracture and lower elongation at break. This phenomenon again confirms from the distinct trends observed in the storage modulus and loss modulus of PI and hybrid films (Fig. 1b and c). Notably, all hybrid films exhibit β-transition temperatures, attributed to the rapid mobility of CF_3 side chains of the CPAF oligomers, while their α-transition temperature derives from the segmental motion of the PI backbone. Interestingly, despite the variations in thermal behavior, the Tg measured *via* dynamic mechanical analyser (DMA) (Fig. 1d) remains nearly identical to that obtained from differential scanning calorimeter (DSC) (Fig. S10 and Table S1, ESI†), highlighting a unique convergence of dynamic and thermal analyses.

Fig. 3 illustrates the dielectric properties of B2FO-CPAF hybrid films as a function of frequency, ranging from 100 kHz to 3 MHz.[16] The ε of PI films is a key parameter for evaluating their insulating properties in electronic and microelectronic applications. As shown in Fig. 3, the ε of PI is reduced by decreasing the density of polar structures, such as the imide ring, through the incorporation of long-chain anhydrides, which lower the molar polarization rate. Additionally, the introduction of bulky and highly electronegative trifluoromethyl groups further lowers ε by disrupting molecular packing, as evidenced by WAXD (Fig. S6, ESI†), and reducing the dipole density per unit volume. However, the ε value of hybrid films decreases with the addition of CPAF, reaching a minimum of 1.58 (at 3 MHz) at 10 wt% CPAF. This represents a significant reduction compared to the ε value of 1.83 for the neat PI film, with the largest decrease being 0.24. This

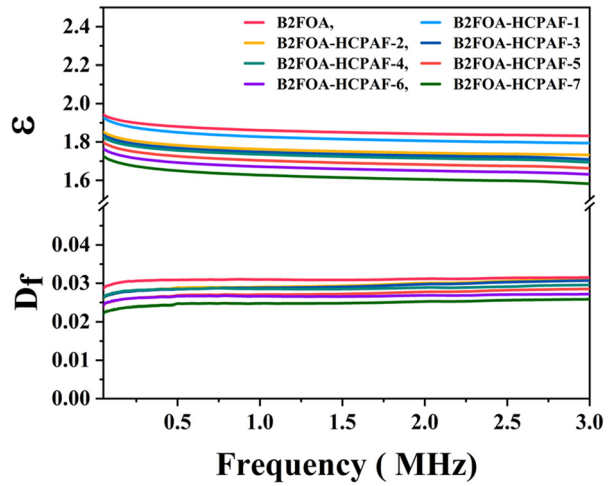

Fig. 3 Dielectric constant (ε) and dielectric loss (D_f) of B2FO PI and B2FO-CPAF PI hybrid films.

reduction indicates that the incorporation of CPAF effectively lowers the dielectric constant of the PI films.[11] The decrease in ε is primarily attributed to the increased fluorine content in the hybrid films. Additionally, CPAF reacts with B2FO chains containing terminal anhydride groups, consuming carboxylic groups from these terminal anhydride functional groups. This reaction suppresses polarization within films, further contributing to the reduced dielectric constant.

The ε value shows a slight decline as the testing frequency increases. Notably, the dielectric constants of the hybrid films exhibit a greater dependency on frequency with increasing CPAF content. This behavior is primarily due to the frequency-dependent polarization mechanism. At higher CPAF contents, an excess of polarizable units exists within the film, leading to varied responses to the applied electric field across different frequencies. The excellent compatibility between PI and CPAF contributes to the improved mechanical and flame-retardant properties observed in this study, which are beneficial for the fabrication of low-dielectric materials.

Conversely, the dielectric loss (D_f) of PI is primarily influenced by dipole depletion under high-frequency electric fields. Incorporating kinkable polyimide systems, such as those containing 1,4-diisopropylbenzene units, reduces electron cloud density, thereby attenuating losses associated with electron movement. Experimental results (Table S2 (ESI†) and Fig. 3) indicate that the D_f of PI at 3 MHz ranges from 0.0245 to 0.0315. Initially, D_f decreases with increasing fluorine content in the PI matrix, indicating enhanced dielectric properties. However, further increases in CPAF content led to non-directional cross-linking and reduced molecular packing within the PI-CPAF hybrids due to the hyperbranched structure of CPAF. This structural change facilitates greater molecular motion, resulting in higher dielectric loss at elevated CPAF levels.

It can be summarized that the deliberate integration of long-chain anhydrides, trifluoromethyl groups, and cross-linking of free PI chains reduces polar density and internal energy dissipation, thereby enhancing the dielectric performance of PI films.

In summary, we successfully synthesized novel PI hybrid films by integrating B2FO PI with a hyperbranched CPAF polymer. The enhanced thermal stability of the PI hybrid films is attributed to reduced thermal vibrations and increased char yield. The improvement in mechanical properties reflects the formation of a robust 3-D network structure, facilitated by crosslinking between PI and CPAF. The incorporation of the hyperbranched CPAF polymer also enhances the water resistance of the PI hybrids through increased fluorine content, while cyclotriphosphazene significantly improves their flame-retardant properties. Additionally, reduced molecular packing and decreased polarization of PI chains collectively contribute to a reduction in dielectric properties. These findings demonstrate the multiple benefits of the synthesized hybrid films for potential applications in the fabrication of microelectronic devices, such as those used in 5G/6G telecommunication.

We are grateful for the financial support from the National Research Foundation of Korea (NRF) Grant funded by the Ministry of Science and ICT, Korea (2021R1I1A3060098).

Data availability

The data supporting this article have been included as part of the ESI.†

Conflicts of interest

There are no conflicts to declare.

Notes and references

1 W. Deng, Y. Shen, J. Qian and H. Yang, *Chem. Commun.*, 2015, **51**(24), 5097.
2 C.-J. Chen, Y.-C. Hu and G.-S. Liou, *Chem. Commun.*, 2013, **49**(25), 2536.
3 S. Zhang, X. Zhao, B. Li, C. Bai, Y. Li, L. Wang, R. Wen, M. Zhang, L. Ma and S. Li, *J. Hazard. Mater.*, 2016, **314**, 95.
4 S. R. Nagella, K. S. V. Krishna Rao, S. Eswaramma and K. Madhusudana Rao, *Polym. Adv. Technol.*, 2016, **27**(3), 374.
5 R. Revathi, P. Prabunathan and M. Alagar, *Polym. Bull.*, 2019, **76**(1), 387.
6 X. Wu, G. Jiang, Y. Zhang, L. Wu, Y. Jia, Y. Tan, J. Liu and X. Zhang, *Polymers*, 2020, **12**, 90.
7 M. Zhang, G. Wang, A. Li, X. Wei, F. Li, J. Zhang, J. Chen and R. Wang, *J. Membr. Sci.*, 2021, **619**, 118800.
8 S. Devaraju, M. Selvi and M. Alagar, *Int. J. Polym. Anal. Charact.*, 2018, **23**(1), 29.
9 M. El Gouri, A. El Bachiri, S. E. Hegazi, M. Rafik and A. El Harfi, *Polym. Degrad. Stab.*, 2009, **94**(11), 2101.
10 H. R. Allcock and R. L. Kugel, *JACS*, 1965, **87**(18), 4216.
11 Z. Fan, I. Noh, C. Zhuang, Q. Liu, Y. Wang, H. D. Kim, M. Yue, H. Ohkita and B. Wang, *Eur. Polym. J.*, 2023, **198**, 112383.
12 Y. Zhou, W. Liu, W. Ye, F. Chu, W. Hu, L. Song and Y. Hu, *Chem. Eng. J.*, 2024, **482**, 148867.
13 S. R. Nagella, S. S. Park, R. K. Chitumalla, J. Jang and C.-S. Ha, *Polym. Int.*, 2024, **73**(3), 238.
14 F. Radmanesh, G. Bargeman and N. E. Benes, *J. Membr. Sci.*, 2023, **668**, 121215.
15 W. Wei, X. Huang, X. Zhao, P. Zhang and X. Tang, *Chem. Commun.*, 2010, **46**(3), 487.
16 Y.-Z. Yan, K. Chen, H. R. Moon, S. S. Park and C.-S. Ha, *Eur. Polym. J.*, 2024, **202**, 112655.